Reaction Constants for $Li^7(p,n)Be^7$

RICHARD TASCHEK AND ARTHUR HEMMENDINGER
Los Alamos Scientific Laboratory, Los Alamos, New Mexico

(Received May 5, 1948)

Absolute values for the reaction cross section of $Li^7(p,n)Be^7$ are given for proton energies between 1.86 Mev and 2.5 Mev. Detailed angular distributions and their analyses are presented and the use of the reaction as a variable energy neutron source is discussed.

I. INTRODUCTION

THE experimental work described below is the result of a cooperative effort by many members of the Van de Graaff group at Los Alamos; the names of the members of this group would appear with those of the writers except for length. They are: Dudley Williams,* Richard Christian,** Arthur Schelberg,*** Harold Argo,**** Roland Perry,** Rubby Sherr,† and Howard Kratz.†† The detailed analyses of the angular distributions were developed and carried out by Frederick Reines.

Following the exploratory work of Hanson, Benedict,[1] and others at the University of Wisconsin during 1942, which had established the general trend of cross section, angular distribution, and monoergic nature of the reaction $Li^7(p,n)Be^7$ to proton energies in excess of 3.0 Mev, this source of neutrons was extensively used at Los Alamos with little further investigation of the reaction itself. The detailed study reported below was undertaken to establish precisely the nature of the reaction, since it is one of the most versatile sources of neutrons available.

The compound system Li^7+p has been studied over a considerable energy interval but the complete experimental picture is not yet known. Information is available about the particle reaction[2–7a]

$$Li^7+p\rightarrow He^4+He^4+17.5 \text{ Mev}, \quad (1)$$

the γ-ray emission[8,9]

$$Li^7+p\rightarrow Be^8+\gamma+17 \text{ Mev} \quad (2)$$

with its resonance at 440-kev proton energy, and the inelastic scattering process[10]

$$Li^7+p\rightarrow Li^{7*}+p, \quad (3)$$

$$Li^{7*}\rightarrow Li^7+h\nu(450 \text{ kev}). \quad (4)$$

The reaction considered in the present study is

$$Li^7+p\rightarrow Be^7+n+Q; \quad (5)$$

$$Be^7+e^K \xrightarrow[K \text{ capture}]{43 \text{ day}} Li^{7*}+\eta_0\rightarrow \begin{cases} Li^7+h\nu+\eta_0 & \text{about 10 percent} \\ Li^7+\eta_0 & \text{about 90 percent.} \end{cases} \quad (6)$$

The excited state of Li^{7*} is presumably the same as in the inelastic scattering case.

The first studies of the trend of this reaction with incident proton energy were made by Wells, Haxby, Shoupp, and Stephens[11] who established, according to their energy scale, that the threshold was at 1.86 Mev, giving a $Q=-1.63$ Mev. This value has been used

* Now at Ohio State University, Columbus, Ohio.
** Now at Argonne National Laboratory, Chicago, Illinois.
*** Now at Indiana University, Bloomington, Indiana.
**** Now at Institute for Nuclear Studies, University of Chicago, Chicago, Illinois.
† Now at Princeton University, Princeton, New Jersey.
†† Now at General Electric Laboratories, Schenectady, New York.

[1] A. O. Hanson, CF-618 (1943); D. L. Benedict and A. O. Hanson, CF-638 (1943).
[2] Herb, Parkinson, and Kerst, Phys. Rev. **48**, 118 (1935).
[3] L. J. Haworth and L. D. P. King, Phys. Rev. **54**, 38 (1938).
[4] Rumbaugh, Roberts, and Hafstad, Phys. Rev. **54**, 657 (1938).
[5] Young, Ellett, and Plain, Phys. Rev. **58**, 498 (1940).
[6] Swartz, Rossi, Jennings, and Inglis, Phys. Rev. **65**, 80 (1944).
[7] J. M. Blair and A. O. Hanson, CF-624 (1943).
[7a] Rubin, Fowler, and Lauritsen, Phys. Rev. **71**, 212L (1947).
[8] Hafstad, Heydenburg, and Tuve, Phys. Rev. **50**, 504 (1936).
[9] W. A. Fowler and C. C. Lauritsen, Phys. Rev. **56**, 841 (1938).
[10] Hudson, Herb, and Plain, Phys. Rev. **57**, 587 (1940).
[11] Wells, Haxby, Shoupp, and Stephens, Phys. Rev. **58**, 1035 (1940).

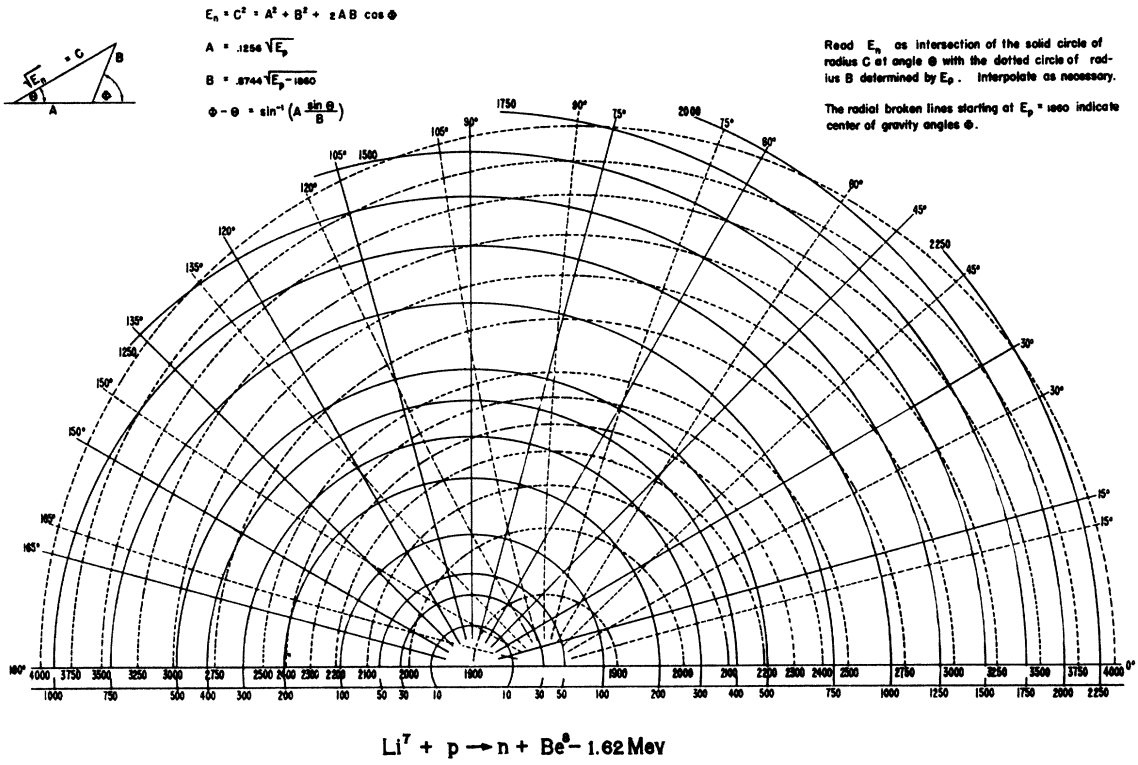

FIG. 1. Energy-angle nomograph for the $Li^7(p,n)Be^7$ reaction.

throughout all the work done at Los Alamos with this source, notwithstanding Hanson and Benedict's[12] value of 1.88_3 Mev at threshold obtained with a curved plate electrostatic analyzer. Recent observations at Los Alamos with a more highly developed electrostatic analyzer[13] corroborate the higher value but further independent methods should be used to clarify this discrepancy.

The other reactions mentioned have not been studied at energies above the threshold for the neutron emission. The question of an excited state in Be^7, which might lead to another group of neutrons at proton energies above some 400 kev above the threshold has not been investigated *per se*, but evidence from proton recoil distributions[14,15] indicates that, up to proton energies of at least 1 Mev above the threshold, no other group than the initial one is present to more than approximately ten percent of the initial group intensity. This excited state is surmised from the expected similarity of the isobars Li^7 and Be^7.

II. SOURCE

In all the work reported below the Los Alamos Van de Graaff generator[13] was used. This machine provides up to 60 μa of magnetically analyzed protons or deterons at a maximum usable energy of 2.7 Mev with an energy control of about ± 1.5 kev and a focus approximately 2 mm in diameter at a distance of 1.5 meters from the analyzing magnet.

Unseparated metallic lithium targets were used for all experiments; these targets, evaporated onto 0.25-mm thick tantalum caps in a separate vacuum system were especially designed to reduce scattering material around the neutron source to a minimum, the 0.25 mm of tantalum being the only material between the lithium film and the outside in the forward direction. For very large proton currents these targets were approximately 3.8 cm in diameter and rotated

[12] A. O. Hanson and D. L. Benedict, Phys. Rev. **65**, 33 (1944).
[13] J. L. McKibben and D. H. Frisch, Phys. Rev. **70**, 117A (1946).
[14] P. G. Koontz and T. A. Hall, LA-128 (1944).
[15] P. G. Koontz and T. A. Hall, MDDC-31 (1946).

eccentrically in a fine air-water spray to dissipate the 100 watts of power, while for currents of 1 or 2 μa small (19 mm in diameter) air-cooled stationary targets were used with no observable loss of lithium as monitored by the neutron flux. The large proton currents available allowed extremely thin (2 to 5 kev) lithium deposits to be used with sufficient neutron yield to make most experiments easily possible. Target thicknesses were measured, for routine work, by the proton energy increment between threshold and the first knee or maximum of the neutron yield at 0°, as measured by a flat energy response counter[16] subtending solid angles as small as 3×10^{-3} steradian (half-angle about 2°) and, subsequent to this, calibration of a counter by the forward yield at 2.05 Mev (see Fig. 3). For the small stationary targets, on which the lithium deposit was very uniform, chemically determined weights were used to measure the surface density of lithium. It was found that carbon deposits made the energy increment method inaccurate for lithium mass determination of the thinnest targets, since the thickness measured in this way grew with time, although for targets thicker than 30 kev the inaccuracy was negligible.

In Fig. 1 is shown an energy-angle nomograph, due to McKibben,[17] for this reaction. This chart will aid in the discussion below since most observations were made on neutrons emerging from the source with different energies because varying proton energies and neutron angles were used. It may be noted here (as can be seen from the nomograph) that for all proton energies, except just at threshold, up to 40 kev above the threshold the neutrons appear double-valued in energy at each angle within a forward cone of less than 2π solid angle; this effect is due to the large center of mass velocity. Above 1.90-Mev proton energy the neutrons have a single energy at each angle and by using large angles (near 120°) experiments may be done with neutrons as low as 5 kev in energy, providing the intensity is sufficient.

Time did not permit an extensive investigation of the angular distribution of neutrons within the double-valued region, but a method using the $N^{14}(n,p)C^{14}$ reaction[18,19] as a detector was devised which appears promising for the resolution of the two groups down to a neutron energy difference of approximately 20 kev, where the neutron energies individually are in the range 2 kev to 100 kev. It will be seen, however, that the ratios of the solid angle factors from center of gravity to laboratory coordinates are in the ratio of the energies of slow to fast groups of neutrons at a given angle (Appendix I); this means that a roughly isotropic distribution in the center of mass system would result in an observationally unfavorable yield for the slow group in the laboratory system, particularly after the cone mentioned above has become large.

Appendix II describes a method of obtaining the energy dependence of a given neutron cross section by taking advantage of the neutron cone in this reaction.

Since the neutrons emerge with varying energies over 4π solid angle, it is highly advisable to keep neighboring scattering and moderating material as far from the source as possible. The present source is located over a pit with a distance of eight feet to ground level, thin fiberboard walls at about twelve feet forward, 2-foot thick concrete walls about ten feet away on either side and, most unfavorably, the edge of the pit about five feet behind the source at four feet above pit floor.

III. REACTION CROSS SECTION

Method

The absolute value of the reaction cross section was determined by a comparison of the total neutron flux from the $Li^7(p,n)Be^7$ source with the total neutron flux from a standardized RaBe source. The source strength for the RaBe source standard was determined by Walker[20] and is known to approximately ±5 percent. From the magnitude of the cross section of $Li^7(p,n)Be^7$ it seems likely that the reverse process could be carried out, i.e., a spectrochemical determination of the mass of Be^7 formed in a long bombardment of a thick Li target would calibrate a RaBe source for neutron flux since approximately 10^{-7} g

[16] A. O. Hanson and J. L. McKibben, Phys. Rev. **72**, 673 (1947).
[17] J. L. McKibben, Phys. Rev. **70**, 101A (1946).
[18] B. T. Feld, Phys. Rev. **70**, 429L (1946).
[19] H. H. Barschall and M. E. Battat, Phys. Rev. **70**, 245 (1946).
[20] R. L. Walker, LA-400 (1945).

of Be^7 can be formed in 48 hours of bombardment (Appendix III).

In the present experiment the fluxes of the two sources were compared at two proton energies, 1.95 Mev and 2.25 Mev, by means of the activities induced in a large "manganese bath." The particular variations in the technique of manganese bath measurements here used were developed and reported in detail by Turner.[21] Briefly, a cubical Lucite container approximately 70 cm on a side contained a solution of 200 g/liter of $MnSO_4$; the 155-minute Mn^{56} activity was excited either by the RaBe source or the $Li^7(p,n)Be^7$ source introduced into the center of the solution on a diagonal of the cube through a horizontal tube of 19-mm diameter. After sufficient exposure of the solution the whole bath was vigorously stirred and approximately a liter of the solution withdrawn in a cylindrical Lucite container. This container was filled to a fixed height, lowered into a lead shield, and a thin-walled (4-mil) Al Geiger counter, carried vertically on the lead lid for the shield, lowered into the solution. The activity was usually followed for more than one half-life with alternate measurements of background being made on a geometrically identical sample of the solution withdrawn before irradiation. Before immersion in the solution, the Geiger counter was thinly coated with ceresin wax to prevent corrosion. The counters were systematically checked for calibration constancy with uranium glass "standards."

Exposures with the RaBe sources used were made for about 12 hours, giving approximately 99 percent saturated activity. Activities induced with the $Li^7(p,n)Be^7$ source required only one or two hours exposure for high counting rates.

It seemed particularly desirable to make total reaction cross-section measurements at closely spaced energies, since the neutron yield was known to vary rapidly with proton energy. Only one, or at most two, exposures of the manganese bath could be made per day, it being necessary to wait for the strong activity from the lithium neutrons to decay considerably before a second run could be made without large corrections. For this reason and the added one of much greater convenience, advantage was taken of the 43-day γ-activity induced in the target itself from decay of the Be^7. The following procedure was adopted:

1. After an exposure of the manganese bath to the $Li^7(p,n)Be^7$ source, which measured directly the total number of neutrons emitted during the course of a run, the bath was rolled off the target and a Geiger counter in a lead shield with a hole and spacer in it for introduction of the target was rolled up to it on a trolley and the Be^7 activity due to the same run measured.
2. In this way, the Be^7 activity counted in a standard geometry was calibrated against the Mn bath and further flux measurements at the same or different proton energies could subsequently be made in terms of the easily measured Be^7 activity rather than by using the cumbersome Mn bath.

For the targets used it had been ascertained that:

1. No Be^7 activity was induced in the Li when protons below the threshold energy of $Li^7(p,n)Be^7$ were used;
2. No activity of any kind was induced in the Ta backing material with protons of energies up to the maximum used in this experiment;
3. No long-lived activity was induced in a block of metallic Li when bombarded with neutrons up to 1-Mev maximum energy;
4. Neither Li nor Ta gave long-lived activities when immersed in slow neutron fluxes corresponding to those met with in the Mn bath for equal lengths of time;
5. The ratios of Be^7 to Mn^{56} activities due to the same run were constant, independent of neutron energies between 30 kev and 1 Mev within experimental error of about six percent.

The last two inches of the small target tubes were made of Ta and at the end of this was the 10-mil Ta cap on which the Li was evaporated. It was found necessary to make this much of the target of Ta to avoid troublesome n, γ-activities induced in such metals as Al, Fe, and Cu when the target was immersed in the strong slow neutron flux of the Mn bath.

It was determined that the small targets were uniformly deposited by making one of these in two annular segments of approximately equal area and analyzing each separately. The chemically determined mass per unit area for the outside ring was within two percent of that of the central disk. Later experience showed, however, that the mass measurements after bombardment on the thinnest targets were not reliable, the error being an approximately constant one and probably a result of the fact that some lithium penetrated rather deeply into the Ta

[21] C. M. Turner, LA-445 (1945).

TABLE I. Mn bath exposures to $Li^7(p,n)Be^7$ source.

E_p (Mev)	Target no.	ρ, surface density of Li in mg/cm²	A_0, Mn^{56} activity at zero time in counts/min.	I, weighted current in μ coul./min.	$A_{Mn}=A_0/I$ in counts/μ coul.	$\sigma_{Li(p,n)}\times10^{24}$ cm² from Eq. (7)
2.25	1	0.105	1675	25.85	64.79	0.508
2.25	2	0.106	963	15.94	60.40	0.470
2.25	2	0.106	3002	47.69	62.94	0.489
						av. 0.489±2.7%
1.95	1	0.105	2201	73.61	29.90	0.234_4
1.95	2	0.106	467	14.66	31.86	0.247_2
1.95	2	0.106	830	28.60	29.02	0.225_5
1.95	3	0.142	940	23.05	40.75	0.236
1.95	3	0.142	1150	28.72	40.10	0.232_3
						av. 0.238±2.8%

E_p (Mev)	Target no.	A_1, Be^7 activity arising from irradiation in counts/min.	Total proton charge q during run in μ coul.	$A_{Be}=A_1/q$ in counts/μ coul.-min.	$R=A_{Mn}/A_{Be}$	A_{Be}/target thickness in counts/min./μ coul. mg/cm²
2.25	1	601	7311	0.0822	788	0.783
2.25	2	320	3958	0.0811	745	0.766
2.25	2	1122	14,005	0.0803	784	0.757
						av. 0.769±4%
1.95	1	1200	29,549	0.0407	735	0.387
1.95	2	171	3632	0.0472	676	0.445
1.95	2	348	8051	0.0432	673	0.407
1.95	3	304	5966	0.0509	801	0.358
1.95	3	382	7598	0.0503	797	0.354
					av. 750±6%	av. 0.390±7.5%

backing material and was not measured in the chemical analysis. This appeared clearly in a series of nine targets bombarded with 2.25-Mev protons for approximately equal times. These targets varied by a factor of 25 between thinnest and thickest in chemically determined mass of lithium. For the targets thicker than 0.08 mg/cm² the Be^7 activity/mg/cm² was independent of the thickness to within the experimental error of ~eight percent in the two measurements and only these targets were used for the absolute comparisons.

In terms of the quantities which are directly measured in the Mn bath experiment, it can readily be shown that the $Li^7(p,n)Be^7$ cross section at the proton energy E is

$$\sigma(E)=\frac{A_0}{A_s}\cdot\frac{[1-\exp(-t_R/\tau)]Q_{RaBe}(1-L)1.983\times10^{-33}}{\sum_i(\Delta q_i/\Delta t_i)[1-\exp(-\Delta t_i/\tau)][\exp(-t_i^*/\tau)]\rho}\ \text{cm}^2, \tag{7}$$

where

A_0 = observed zero time activity of Mn^{56} due to a run on Li(p,n) neutrons (zero time is defined as the end of the irradiation),

A_s = observed zero time activity of Mn^{56} due to RaBe neutrons,

Q_{RaBe} = number of neutrons/minute from the RaBe source,

L = fraction of RaBe neutrons leaking from Mn bath,

t_R = duration of RaBe exposure,

τ = decay period of Mn^{56} = 224.2 minutes,

ρ = surface density of normal lithium on target in mg/cm²,

$T=\sum_i\Delta t_i$ is the total exposure time in a given run to Li(p,n) neutrons,

Δq_i = charge in micro-coulombs due to protons striking the target in sub-interval Δt_i,

t_i^* = time elapsed from end of Δt_i to end of irradiation.

The numerical factor 1.983×10^{-33} is determined by the constants: charge of the proton, Avogadro's number, atomic weight of normal lithium, and the isotopic constitution of lithium.

TABLE II. Standardization of Mn bath.

Run no. and data	Q_{RaBe} source strength in n/min.	t_R exposure length in min.	A_s bath activity at zero time in c/min.	k bath constant in counts/neutron
1 (4–9–46)	5.37×10^8	1369	1210	2.33×10^{-6}
2 (4–17–46)	5.37×10^8	1566	1220	2.35×10^{-6}
3 (4–20–46)	3.48×10^8	1347	802	2.39×10^{-6}
4 (5–16–46)	3.48×10^8	1600	869	2.57×10^{-6}
				$k_{Av}=2.41\times10^{-6}\pm3\%$

IV. MEASUREMENTS

In Eq. (7) the summation is necessary because over the whole irradiation time T it was difficult to keep the proton current sufficiently constant to use simply the induced activity per microcoulomb derived from dividing the infinite exposure activity by the total charge from the protons during the run. The summation is over the proton current to the target during short intervals suitably weighted to account for bath decay during irradiation. Thus, in Table I, which gives the results of the eight Mn bath measurements on the $Li(p,n)$ source, the quantity

$$A_{Mn}=\frac{A_0}{\sum_i(\Delta q_i/\Delta t_i)[1-\exp(-\Delta t_i/\tau)][\exp(-t_i^*/\tau)]}=\frac{A_0}{I} \tag{8}$$

is the infinite exposure specific activity of the Mn bath and is independent of duration or intensity of the irradiation on a given target at a fixed proton energy.

In Table II are shown the individual Mn bath standardizations obtained with the two different secondary standard RaBe sources used which determine the bath constant

$$k=A_s/Q_{RaBe}(1-L). \tag{9}$$

The leakage factor L used was 0.03, based upon early calculations of RaBe spectrum leakage corrected for new bath size and revised estimate of the spectrum; whatever errors are in this estimate are considerably smaller than the remainder of the experimental errors. It will be noted that the last calibration was done at the end of the Mn bath experiment and, in its deviation from the other three runs, may indicate a small change in bath constant during this time; since the effect was small, no correction was made. For the four runs the average value of k in counts per neutron was $2.41\times10^{-6}\pm3$ percent.

For the data taken by the Be^7 method, the

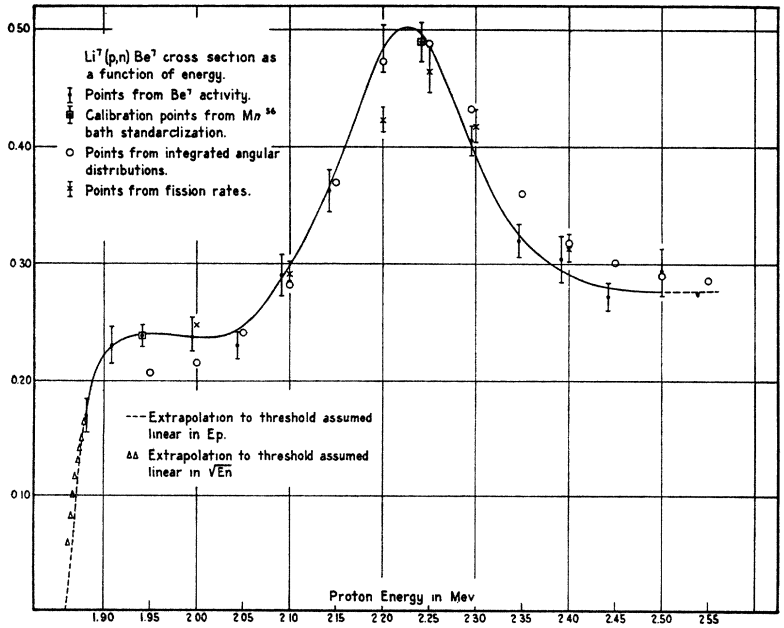

FIG. 2. $Li^7(p,n)Be^7$ reaction cross section in units of 10^{-24} cm² as a function of proton energy.

cross sections obtained for target thicknesses above 0.08 mg/cm² were consistently reliable, while for much lighter targets the chemical weights were untrustworthy. However, for almost all targets at least one measurement of the activity for an exposure at $E_p = 2.25$ Mev, the standardization energy, was made. In this case, the ratio of Be^7 activity at any energy above threshold to that of 2.25 Mev was completely independent of target thickness and excellent agreement was obtained in all cases.

The total $Li^7(p,n)Be^7$ cross section thus obtained is shown in Fig. 2. The proton energies at which the cross sections are plotted are corrected for target thickness, which varied from 5 to 20 kev. The errors shown on the Be^7 points are the mean deviations of two or more runs at the given energy.

In the same figure the circles are data obtained by integration of the angular distributions discussed in the next section and normalized to the Mn bath data at 2.25 Mev. These data will be discussed in more detail in the next section; the errors are estimated to be about ±5 percent except at the lowest energies where they may be larger, due to changes in detector sensitivity and background.

The crosses in Fig. 2 represent data taken with a U^{235} fission foil subtending a half-angle of 18° at the zero degree position. From the known weight and cross sections of the U^{235}, and the angular distributions of the next section which gave the fraction of all the neutrons emitted causing the measured fission rate, the cross section of the $Li^7(p,n)Be^7$ reaction was calculated assuming a target thickness of 0.012 mg/cm². This target thickness cannot be more than an estimate, since it was obtained from a rise curve which will be discussed in more detail in the next section, but the agreement is fairly good in absolute value. The errors here indicated are the statistical errors in the fission counts.

The absolute value of the $Li^7(p,n)Be^7$ cross section is good to about ±12 percent over-all; this arises from an estimated ±5 percent error in mass determination, ±6 percent in absolute source strength of the secondary RaBe standards, and about ±2 percent in activity measurements. The relative values of the cross section as a function of energy are somewhat better than this and the curve drawn through the Be^7 points is estimated to be good to ±6 percent at individual points.

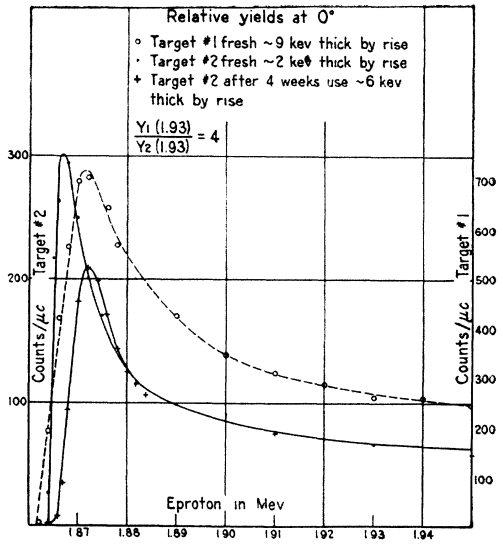

FIG. 3. Neutron yields in the forward direction as a function of proton energy for different target thicknesses.

V. ANGULAR DISTRIBUTION

Method

The angular distribution of the neutrons from the $Li^7(p,n)Be^7$ reaction was measured with a counter, whose response was nearly independent of neutron energy, over a range of proton energies from 1.95 Mev to 2.25 Mev in 50-kev steps. The same rotating target was used for all these measurements, and a second (monitor) counter similar to the one mentioned above was kept at zero degrees to the beam in order to be sure that no systematic changes in neutron flux occurred. The movable counter subtended a solid angle of 1.06×10^{-2} steradian (half-angle approximately 3.5°) and the monitor an angle of 0.32×10^{-2} steradian (half-angle approximately 2°).

A very thin target was used in order to get maximum resolution in the angular distribution data. In Fig. 3 is shown a plot of the forward yield of neutrons for two targets near threshold as measured by the monitor counter. The curves for both targets show the yield and rise-width thickness ratios to be the same while both targets are fresh, but after four weeks' use of target 2 in the angular distribution measure-

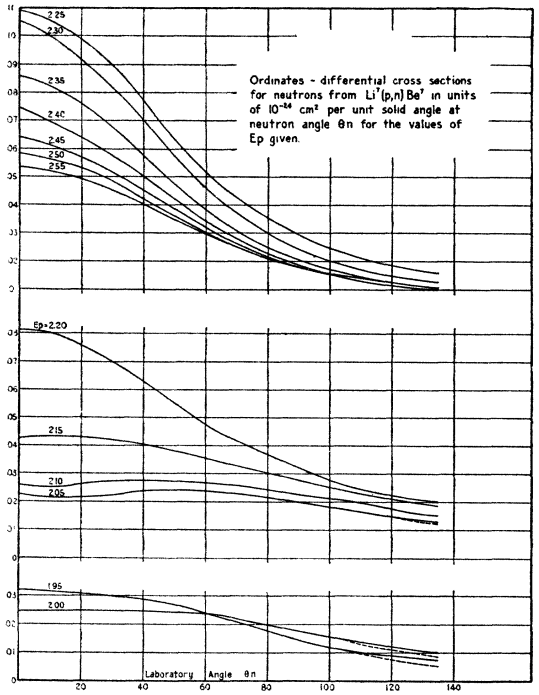

FIG. 4. Laboratory angular distributions in 10^{-24} cm² per unit solid angle as a function of laboratory angle at the listed proton energies.

ments, the yield ratio at 1.93 Mev is still the same but the rise-width has increased from about 2 kev to an apparent 6 kev. Since the yield at the flat portion of the curve remained the same, no lithium was lost or gained and the increased rise width was due to an inert contaminant, undoubtedly a carbon deposit.

Since changing angles was less convenient than changing energies, the movable counter was set at a fixed angle and the yield at that angle was measured as the energy was changed from 1.95 Mev to 2.55 Mev in 50-kev steps. In this manner the angular range from 0° to 135° was covered in approximately 15° intervals.

Serious difficulties were expected at 135° for the lowest proton energies. Two background effects at 1.95 Mev and 2.00 Mev may interfere with the direct neutrons at 135°, since the yield of neutrons here is small compared to those going at the same time in the forward direction. One of these effects is due to room and floor scattering, the other to direct back scattering with little energy loss from the target backing material. The latter effect was determined to be negligible for the present backing material of 10-mil Ta, by observing that approximately 1 cm of Ta in addition to the target cap was necessary immediately in front of it before an appreciable change in counting rate was made at 135°.

The effect of the sea of scattered and degraded neutrons was determined by observing the deviation from r^{-2} dependence of intensity on distance from the source. This type of measurement was first done at a forward angle (65°) to locate the "effective center" of the counter, since here the direct neutron flux completely overshadows backgrounds at the distances involved and the counter length is an appreciable fraction of the closest distances to the source. The intercept of the linear counting rate curve plotted against r^{-2} gave the background counting rate correction necessary at the distance where the angular distribution measurement was made. Corrections were necessary only at 135° and at the proton energies 1.95, 2.00, and 2.05 Mev; the corrected yields were, respectively, 68 percent, 83 percent, and 93 percent of the observed.

A further correction to the yields at 135°, for the lowest proton energies, should have been made for change in counter sensitivity. The neutron energies here are between 15 and 25 kev and previous experience with this type of counter has indicated that a loss in sensitivity of at least 10 percent is quite usual at these energies. However, since no actual sensitivities for these particular counters had been determined, no correction has been made. It is believed that the sensitivities of the two counters used is independent of neutron energy to ± 5 percent in the energy range from about 50 kev to 850 kev, the maximum energy occurring in this experiment.

VI. RESULTS

In Fig. 4 are shown the angular distributions as measured in the laboratory coordinate system. The cross section is given in 10^{-24} cm² per unit solid angle for neutrons at the neutron angle in question. This has been done by calculating, from the measured angular distribution, the fraction of all the neutrons passing through the counter at 0° and 2.25 Mev, where the Mn bath absolute cross section was measured, and normalizing the observed counting rate to the

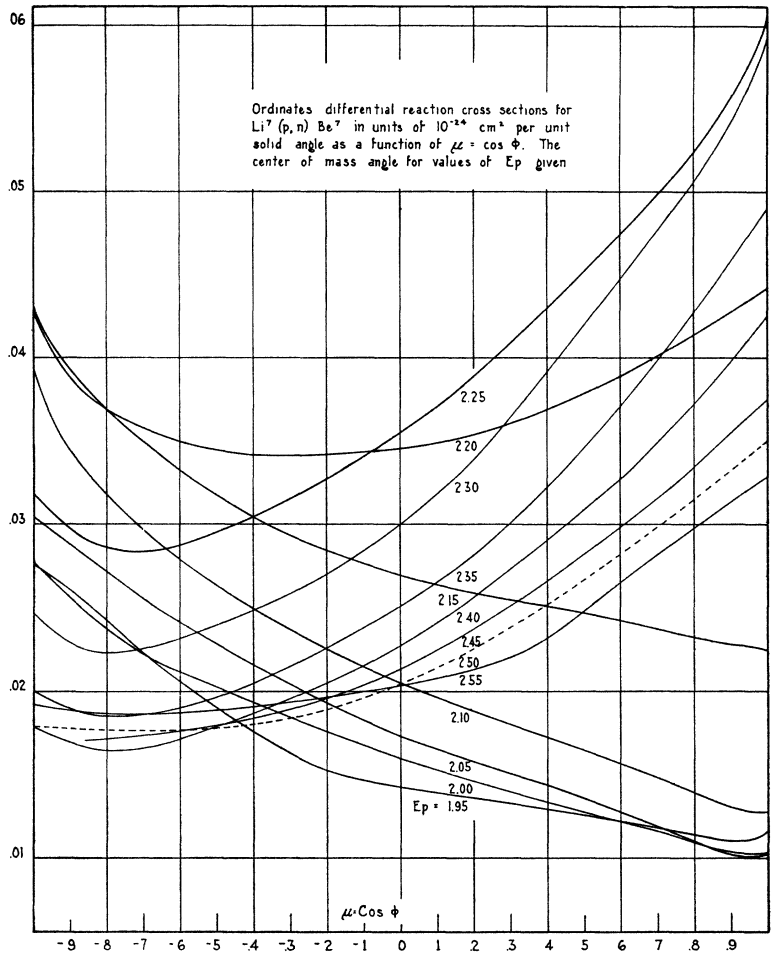

FIG. 5. Angular distributions in the center of mass system in units of 10^{-24} cm² per unit solid angle as a function of the cosines of the center of mass angle at the listed proton energies.

differential cross section obtained from the fraction and the total cross section.

From Fig. 4 it is immediately apparent that although the total cross section is not exceedingly large, the strong forward asymmetry of neutron yield, which comes primarily from center of mass motion at low neutron energies and from the effect of the resonance at high energies, makes this a particularly strong neutron source for forward observations.

Figure 5 shows the center of mass differential cross sections as a function of the cosine of the center of mass angle. Laboratory system yields were converted to center of mass by means of the following relationships holding for the $Li^7(p,n)Be^7$ reaction:

$$\phi=\theta+\sin^{-1}(\sin\theta/\gamma), \tag{10}$$

$$\gamma=7((E_p-E_{th})/E_p)^{\frac{1}{2}}, \tag{11}$$

$$\sigma(\phi)\sin\phi d\phi=\sigma(\theta)\sin\theta d\theta, \tag{12}$$

where ϕ = neutron angle in the center of mass system, θ = neutron angle in the laboratory system, E_p = energy of the incident proton, E_{th} = energy of the incident proton at the threshold; $d\Omega_{lab}/d\Omega_{cm}=\sin\theta d\theta/\sin\phi d\phi$ = ratio of solid angles in center of mass system to that in the laboratory system. For 0° and 180°

$$\frac{d\Omega_{lab}}{d\Omega_{cm}}=\frac{\gamma(\gamma^2-\sin^2\theta)^{\frac{1}{2}}}{\gamma^2+\cos2\theta+2\cos\theta(\gamma^2-\sin^2\theta)^{\frac{1}{2}}}. \tag{13}$$

For all other angles

$$d\Omega_{lab}/d\Omega_{cm}=\cos(\phi-\theta)(\sin\theta/\sin\phi)^2. \tag{14}$$

The angular distributions in the center of mass system can be accurately fitted with a simple power series of the form

$$\sigma(\phi)=A(E)+B(E)\cos\phi+C(E)\cos^2\phi, \tag{15}$$

but a more adequate representation in terms of Legendre polynomials has been devised. This

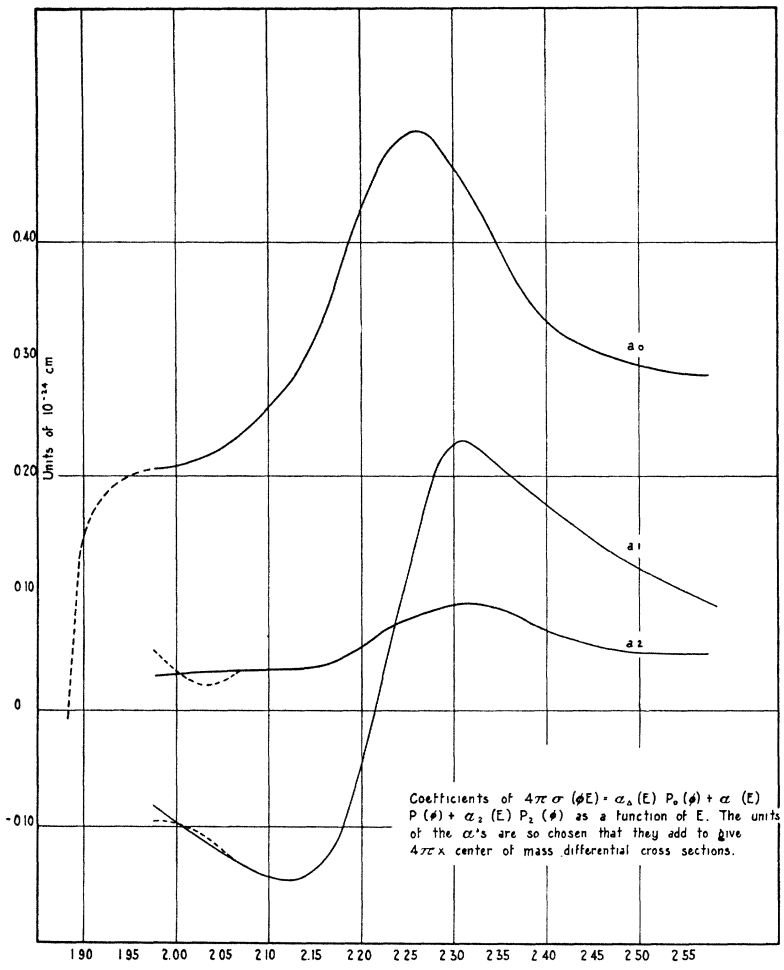

FIG. 6. Energy dependence of the coefficients a_0, a_1, and a_2 of the Legendre polynomial fit to the center of mass angular distributions. The units of the a's have been adjusted to give 4π times the center of mass differential cross sections, at a chosen value of ϕ and E_p.

method has the great advantage of giving a fit to the data which is insensitive to the exact shape of the curve, and therefore to experimental errors, since it depends on the integral properties of the curve when advantage is taken of the orthogonal nature of the functions. Moreover, the resolution of the data is immediately into the partial waves of which the emitted wave may be assumed to be composed. For this method of analysis

$$\sigma(\cos\phi, E) = a_0(E)P_0(\mu) + a_1(E)P_1(\mu) + a_2(E)P_2(\mu), \quad (16)$$

where $\mu = \cos\phi$ and $P_i(\mu)$ is the Legendre polynomial of order i. The derivation of this expansion and its use in determining the energy dependent coefficients are given in Appendix IV.

The coefficients a_0, a_1, and a_2 are plotted in Fig. 6 as a function of the proton energy. It is immediately apparent that the energy dependence is a resonance process. From the analysis $2a_0(E)$ is the total cross section for the process and there is good agreement between this curve and the one from the Be^7 method except at the very lowest energies (see Fig. 2) where it is believed the angular distribution measurements are most inaccurate.

It would be of considerable interest to investigate how the coefficients a_0, a_1, and a_2 approach the threshold below 1.95 Mev, the lowest energy studied here. There is some indication that a_1 and a_2 are approaching zero as threshold is approached but there are no experimental data to support this; a_0 should be proportional to total cross section for which Be^7 measurements were made down to 1.883 Mev. Below this energy

total yield measurements are difficult of interpretation since target thicknesses must be held to a minimum. At the high energy of the threshold for this reaction it does not seem necessary that the P wave be zero at threshold. Since the lowest energy Be^7 measurement gave a yield only about 70 percent of the next at 25-kev higher energy, it seemed reasonable to extrapolate the total yield to zero at threshold.

The curves of forward yield in Fig. 3 show such a sharp rise just above threshold that there may be some question of a resonance there in the reaction yield. One might expect that very near threshold the cross section would be proportional to the neutron velocity in the center of mass system. Figure 7 shows a plot of $\sigma/(E_n)^{\frac{1}{2}}$ as a function of $(E_n)^{\frac{1}{2}}$ where $(E_n)^{\frac{1}{2}}$ is proportional to the neutron velocity in the center of mass system. The solid portion of this curve is drawn through points obtained from the actual data taken above 1.883 Mev. Below this the dotted curves arise from the two extrapolations of the data to zero at threshold shown in Fig. 2 between 1.860 and 1.883 Mev. It is seen that $\sigma/(E_n)^{\frac{1}{2}}$ is very sensitive to the exact extrapolation and the dependence of σ on $(E_n)^{\frac{1}{2}}$ must wait on very precise data in this region.

Although the possibility of a resonance near threshold is thus not ruled out, the general trend of the total yield makes it seem unlikely or weak. The rapid decrease in forward yield may be explained by the center of mass motion, which makes the neutrons come out in a cone near threshold, the solid angle included in the cone increasing more rapidly than ΔE_p, the proton energy increment above threshold. Thus the function

$$\frac{\Delta E_p}{1-\cos\theta_{\text{cone edge}}}$$

is rather rapidly decreasing and the forward yield will go down as this ratio if the total yield is proportional to ΔE_p. In addition to this, the angular distribution in the center of mass system may be such as to reduce the forward yield. Even for a spherically symmetric yield in the center of mass system, the solid angle factor alone will reduce the laboratory yield in the forward direction as ΔE_p becomes larger, since ratio of solid angles of slow to fast group decreases in the same way as the ratio of the energies of these groups.

We wish to thank Mr. William Ashley of the analytical chemistry group for his work on the weight analysis of the many lithium targets used.

This paper is based on work performed under U. S. Government Contract No. W7045-eng 36 at the Los Alamos Scientific Laboratory of the University of California.

APPENDIX I

Energy and Angle Relationships in Double Group Region

Using Eqs. (10), (11), and (13),

$$E_n(\theta)=(E_p/64)(\gamma^2+2\gamma\cos\phi+1)$$

gives the energy in the laboratory system as a function of the center of mass angle ϕ. Then for $\theta=0°$ and $\phi=0°$, i.e., for the *fast* group:

$$E_n{}^F(0°)=(E_p/64)(\gamma+1)^2,$$

and for $\theta=0°$, $\phi=180°$ which occurs only near threshold and results in the *slow* group:

$$E_n{}^S(0°)=(E_p/64)(\gamma-1)^2,$$

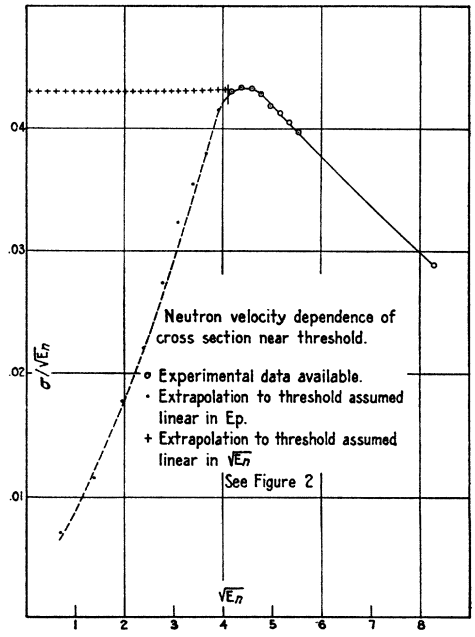

FIG. 7. Reaction cross section as a function of neutron velocity in the center of mass system extrapolated to threshold according to linear or quadratic dependence of σ on E_p.

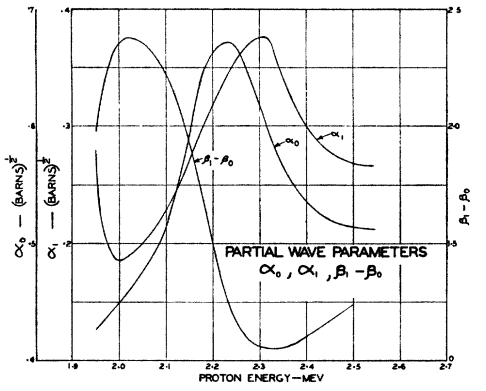

FIG. 8. Partial wave parameters α_0, α_1, and $\beta_1-\beta_0$ as a function of energy.

and the solid angle factor for 0° observation is

$$\Omega_S/\Omega_F=(\gamma-1)^2/(\gamma+1)^2=E_S/E_F.$$

This solid angle factor varies from unity just at threshold to as little as 0.01 at energies where the cone angle is large. At the edge of the cone, however, there is always only one energy neutron present.

APPENDIX II

A 30-Kev Neutron Source

The following method of measuring a cross section for 30-kev neutrons if the cross section is known for a higher neutron energy is a result of the special properties of the $Li^7(p,n)Be^7$ reaction and has been used successfully to measure cross sections.

If the bombarding proton energy is set very close to threshold of the reaction, small energy fluctuations will produce bursts of neutrons of very nearly 30 kev in energy, all lying within a very narrow cone. This cone opens to only 40° half-angle at 16 kev above threshold so that a thin foil or thin gas-filled counter of the element, for which the low energy cross section is desired, placed as close as possible to the essentially point source will always receive the *total* neutron yield from the source. If now the foil has a uniform surface density (this is always true for a gas counter) and the total neutron yield is monitored by the Be^7 activity, the ratio of the cross section at this energy to the cross section for, say, 1 Mev neutrons is found. For the 1-Mev neutrons the cross section must be known and the angular distribution of the neutrons measured, since here the Be^7 activity monitors total flux while the counter receives only a fraction of this. Often the angular distribution for the case where the $Li^7(p,n)Be^7$ reaction gives 1-Mev neutrons at zero degrees can be done with the detector in question since the minimum neutron energies at this proton energy are still about 400 kev.

APPENDIX III

Amount of Be^7 Formed

At a bombarding energy of 2.6 Mev a thick target density will be approximately 6 mg/cm²; a slightly thicker target should be used so that forward Be^7 recoils will not hit the backing material. Assuming an average cross section of 0.3 barn, which is conservative, and a mean energy loss of the protons in the lithium of 130 kev per mg/cm², also conservative, one finds

$$\frac{\text{No. } Be^7 \text{ atoms formed}}{\text{Microcoulomb}}\cong 6.25\times10^{12}\times0.3\times10^{-24}\times5.7\times\frac{6.03}{7}\times10^{20}$$

$$=9.2\times10^{8}.$$

On the Los Alamos machine a 50 μa beam can easily be maintained for long periods of time; thus 48 hours of exposure would give 8.0×10^{15} atoms or 0.09 microgram of Be^7 formed, neglecting decay. Because of the 43-day half-life this exposure may be made over several days period, the decay rate being only about 1.6 percent per day, for which corrections can be accurately made.

Spectrochemical techniques seem capable of determining Be to an accuracy of five percent in concentrations of less than one part per million. If this accuracy can be slighly improved, this would provide a straightforward method of measuring the total flux of neutrons from the source during such an exposure. In particular, manganese bath activities taken over selected portions of such a run would then be standardized and RaBe source strengths could be measured in terms of their activities induced in the same bath. If chemical separation of Be from the bulk of the Li is necessary, the ratio of Be^7 activities in two

samples allows a simple determination of the separation efficiency.

APPENDIX IV

Method of Analysis of Angular Distributions

The method developed below is due to Frederick Reines of the Theoretical Division.

The observed neutron intensity $I(\mu, E)$ in the center of mass system is plotted as a function of $\mu=\cos\phi$ at each proton energy E.

At a given energy E, the amplitude of the neutron wave is

$$f(\mu)=\sum_{i=0}^{m} a_i P_i(\mu), \tag{1}$$

where P_i is the Legendre polynomial of the first kind and $a_i=\alpha_i \exp[i\beta_i]$. Then

$$I(\mu)=|f(\mu)|^2=\sum_{\substack{i=0\\ i\neq j}}^{m}\sum_{j=0}^{m} a_i P_i(\mu) a_j^* P_j(\mu). \tag{2}$$

In terms of α_i and β_i this becomes

$$I(\mu)=\sum_{\substack{i=0\\ i\neq j}}^{m}\sum_{j=0}^{m}\alpha_i\alpha_j\cos(\beta_i-\beta_j)P_iP_j+\sum_{i=0}^{m}\alpha_i^2P_i^2, \tag{3}$$

and using the theorem

$$P_iP_j=\sum_{r=0}^{i} C_r P_{i+j-2r}, \quad i\geq j, \tag{4}$$

where

$$C_r=(A_{i-r}A_rA_{j-r}/A_{i+j-r})\cdot(2i+2j-4r+1)/(2i+2j-2r+1),$$

$$A_r=[1\cdot3\cdot5\cdots(2r-1)]/r!,$$

it is possible to write $I(\mu)$ as a *linear* expansion in the P's instead of products. Thus

$$I(\mu)=\sum_{\substack{i=0\\ i\neq j}}^{m}\sum_{j=0}^{m}\alpha_i\alpha_j\cos(\beta_i-\beta_j)\sum_{r=0}^{i}C_rP_{i+j-2r}+\sum_{i=0}^{m}\alpha_i^2\sum_{r=0}^{i}C_rP_{2(i-r)}, \tag{5a}$$

and by collecting coefficients,

$$I(\mu)=a_0P_0+a_1P_1+\cdots+a_mP_m.$$

From the orthogonality properties of the Legendre polynomials one finds

$$\int_{-1}^{+1} IP_n d\mu=\sum_{i=0}^{m}[2\alpha_i/(2i+1)]=a_0 \quad \text{for} \quad n=0 \tag{6a}$$

$$=[2/(2n+1)]\left\{\sum_{\substack{i=0\\ i\neq j}}^{m}\sum_{j=0}^{m}\alpha_i\alpha_j\cos(\beta_i-\beta_j)C_{[(i+j-m)/2]}+\sum_{i=0}^{m}\alpha_i^2C_{i-(m/2)}\right\} \quad \text{for} \quad n\neq0$$

$$=a_n[2/(2n+1)].$$

Thus from the plot of the experimental $I(\mu)$ one can immediately calculate the coefficients from

$$a_n=[(2n+1)/2]\int_{-1}^{+1} IP_n d\mu, \tag{7}$$

without recourse to the *detailed* shape of the curve.

For the present data the calculations were carried out through a_6; however, all coefficients beyond a_2 were zero to within the experimental error of <6 percent, i.e. only S and P waves were sufficient to describe the distributions up to 2.55 Mev.

In terms of the α's and β's the coefficients are

$$a_0(E)=\alpha_0^2(E)+\alpha_1^2(E)/3,$$
$$a_1(E)=2\alpha_0(E)\alpha_1(E)\cos(\beta_1-\beta_0),$$
$$a_2(E)=\tfrac{2}{3}\alpha_1^2(E),$$

and the total cross section is given by $2a_0$. Curves are shown in Fig. 8 for the energy dependence of the partial wave parameters α_0, α_1, and $\beta_1-\beta_0$.

It should be noted that in the case in which an admixture of more than S and P waves is required to describe the distribution there are more unknowns than equations, rendering impossible a unique assignment of amplitudes and phases.